APPLIED AND ENVIRONMENTAL MICROBIOLOGY, Sept. 2003, p. 5483–5491 Vol. 69, No. 9
0099-2240/03/$08.00+0 DOI: 10.1128/AEM.69.9.5483–5491.2003

Identification of Methyl Coenzyme M Reductase A (*mcrA*) Genes Associated with Methane-Oxidizing Archaea

Steven J. Hallam,[1] Peter R. Girguis,[1] Christina M. Preston,[1] Paul M. Richardson,[2] and Edward F. DeLong[1]*

Monterey Bay Aquarium Research Institute, Moss Landing, California 95039-9644,[1] and The Joint Genome Institute, Walnut Creek, California 94598[2]

Received 28 March 2003/Accepted 25 June 2003

Phylogenetic and stable-isotope analyses implicated two methanogen-like archaeal groups, ANME-1 and ANME-2, as key participants in the process of anaerobic methane oxidation. Although nothing is known about anaerobic methane oxidation at the molecular level, the evolutionary relationship between methane-oxidizing archaea (MOA) and methanogenic archaea raises the possibility that MOA have co-opted key elements of the methanogenic pathway, reversing many of its steps to oxidize methane anaerobically. In order to explore this hypothesis, the existence and genomic conservation of methyl coenzyme M reductase (MCR), the enzyme catalyzing the terminal step in methanogenesis, was studied in ANME-1 and ANME-2 archaea isolated from various marine environments. Clone libraries targeting a conserved region of the alpha subunit of MCR (*mcrA*) were generated and compared from environmental samples, laboratory-incubated microcosms, and fosmid libraries. Four out of five novel *mcrA* types identified from these sources were associated with ANME-1 or ANME-2 group members. Assignment of *mcrA* types to specific phylogenetic groups was based on environmental clone recoveries, selective enrichment of specific MOA and *mcrA* types in a microcosm, phylogenetic congruence between *mcrA* and small-subunit rRNA tree topologies, and genomic context derived from fosmid sequences. Analysis of the ANME-1 and ANME-2 *mcrA* sequences suggested the potential for catalytic activity based on conservation of active-site amino acids. These results provide a basis for identifying methanotrophic archaea with *mcrA* sequences and define a functional genomic link between methanogenic and methanotrophic archaea.

Anaerobic methane production and consumption play critical roles in carbon cycling in marine sediments (26). These processes are enabled by related groups of methanogenic archaea and methane-oxidizing archaea (MOA) (reviewed in references 31 and 32). All known methanogens express the enzyme methyl coenzyme M reductase (MCR), which catalyzes the terminal step in biogenic methane production (reviewed in references 8, 27, and 30). Currently the presence of MCR is considered a diagnostic indicator of methanogenesis (8, 16, 18, 27, 30). The genomes of all methanogenic archaea encode at least one copy of the *mcrA* operon (reviewed in reference 7, 27, 30). Composed of two alpha (*mcrA*), beta (*mcrB*) and gamma (*mcrG*) subunits, the *mcrA* holoenzyme catalyzes heterodisulfide formation between coenzyme M and coenzyme B from methyl-coenzyme M and coenzyme B and the subsequent release of methane (5). Functional constraints on its catalytic activity have resulted in a high degree of MCR amino acid sequence conservation, even between phylogenetically distant methanogenic lineages (18, 27). This conserved primary structure has been used to develop degenerate PCR primers for recovering naturally occurring *mcrA* fragments from a variety of environments (16, 18). The resulting *mcrA* sequence data have been employed as a proxy for methanogen diversity (16, 18).

* Corresponding author. Mailing address: Monterey Bay Aquarium Research Institute, 7700 Sandholdt Rd., Moss Landing, CA 95039. Phone: (831) 775-1843. Fax: (831) 775-1620. E-mail: delong@mbari.org.

Diagenetic modeling and geochemical studies have predicted and identified the process of anaerobic methane oxidation in anoxic marine environments (1, 14, 19, 25, 26, 33). Subsequent culture-independent biochemical and molecular studies revealed the lipid biomarker and genetic signatures of methanogen-related archaeal communities associated with anaerobic methane oxidation (4, 12, 21–24). Currently no archaeon capable of anaerobic methane oxidation has been isolated in pure culture, but coupled fluorescent in situ hybridization and isotopic analysis have linked two specific groups of MOA, ANME-1 and ANME-2, to the process of anaerobic methane oxidation (22). The specific molecular mechanisms underlying anaerobic methane oxidation remain obscure. One possibility suggested by phylogenetic and biochemical considerations is that MOA have co-opted the methanogenic pathway, reversing key steps to enable methane oxidation anaerobically. To begin testing this hypothesis, we attempted to isolate *mcrA* genes from MOA by a variety of approaches, including PCR surveys of naturally occurring populations, enrichment cultures, and genomic library screening.

MATERIALS AND METHODS

Site description and sampling. Sediment push cores were collected at Eel River Basin with the ROV *Ventana* and at Monterey Canyon with the ROV *Tiburon*. Benthic sediments collected from Monterey Bay were incubated for 24 weeks on a continuous-flow anaerobic sediment incubator (AMIS) (10a). The AMIS incubator was designed to provide anaerobic, methane-saturated, sulfate-containing seawater to the sediments to foster the enrichment of MOA. Enrichments with the AMIS bioreactor led to the growth of MOA in both sediments collected from seeps (seep sediments) as well as sediments collected away from

TABLE 1. Sample origin and environmental data

Location and sample type	Sample	Core depth (cm)	Water depth (m)	Coordinates (°N, °W)	Description
Eel River	T201	4–7	550	40.48, 124.36	Clam patch, high CH_4 fosmid library
	GZfos				
Monterey Canyon					
Seep	F17.1	0–25	955	36.77, 122.08	Clam patch, high CH_4
Nonseep	C4.1				AMIS microcosm[a]
Blake Ridge	PC26	76	2,707	31.53, 75.45	Hemipelagic sediment

[a] AMIS microcosm cultured from nonseep reference core collected at least 25 m away from any known seep site.

seeps (nonseep sediments). Prior to AMIS incubation, MOA were not detected in nonseep sediment following small-subunit (SSU) 16S rRNA-directed PCR screening and in situ hybridization with MOA group-specific probes (10a). After incubation, MOA were detectable, and 1-g subsamples of these incubated sediments were taken for analysis in this study. Piston cores were collected at Blake Ridge off the R/V *Cape Hatteras*. For microbiological analysis, 0.5 g of sediment was diluted in 1 ml of 1× phosphate-buffered saline–ethanol and stored at −20°C until processed.

Sediment DNA extraction. From 0.25 to 0.5 g of sediment in 1× phosphate-buffered saline–ethanol was diluted in 1500 μl of 1× phosphate-buffered saline and sonicated for 30 s at 30 A (Sonics and Material Inc., Danbury, Conn.) on ice. Samples were layered over a 50% Percoll (Sigma)–1× phosphate-buffered saline continuous gradient and centrifuged for 15 min at 4,800 rpm in an HS-4 rotor at 4°C. DNA for subsequent PCR amplification was extracted from sediment pellets following Percoll gradient centrifugation with a Fast soil prep kit (MoBio, San Diego, Calif.). Final elution volumes varied between 30 and 50 μl of TE (10 mM Tris, 1 mM EDTA, pH 7.5).

Fosmid library construction and screening. Fosmids were prepared by a modification of a previously described protocol (28). Pooled supernatant from 10 g of Eel River T201 Percoll layered sediment was filtered onto 3-μm-pore-size polycarbonate filters and either frozen at −20°C or processed immediately for high-molecular-weight DNA extraction (Hallam et al., unpublished data). Briefly, high-molecular-weight DNA was end-repaired and separated on 0.8% agarose in 1× TAE overnight at 30 V. Then 40- to 50-kb fragment pools were gel purified and cloned into the vector pEpiFOS (Epicentre) according to the manufacturer's instructions. Ligated DNA was packaged with the Epicentre MaxPlax lambda packaging extract and used to transfect *Escherichia coli* DH10B cells (Bethesda Research Laboratories). Transfected cells were selected on Luria-Bertani (LB) agar containing chloramphenicol.

The resulting clones were picked into 96-well (n = 37) microtiter dishes containing LB supplemented with chloramphenicol and 7% glycerol and stored at −80°C. For screening purposes each 96-well plate was individually pooled, and plasmid DNA was extracted by standard alkaline lysis procedures (28). Fosmid subclone libraries were generated with the Topo Shotgun kit (Invitrogen, Carlsbad, Calif.). Briefly, high-molecular-weight DNA was nebulized to 1 to 3 kb, end-repaired, and cloned into the Topo blunt-end cloning vector pCR4. Ligated DNA was used to transform electrocompetent *E. coli* Top10 cells. Transformants were selected on LB containing 50 μg of kanamycin per ml under blue-white selection. The resulting clones were robotically picked at the Joint Genome Institute into 384-well microtiter dishes containing LB with 50 μg of kanamycin per ml plus 7% glycerol and stored at −80°C.

SSU rRNA and *mcrA* gene amplification. SSU rRNA sequences were PCR amplified from environmental and fosmid DNA extracts with archaeon-specific primers A20_F (5′-TTCCGGTTGATCCYGCCRG) and A958_R (5′-YCCGG CGTTGAMTCCAATT). *mcrA* group a and c to e sequences were PCR amplified with universal *mcrA* primers ME1 (5′-GCMATGCARATHGGWATGTC) and ME2 (5′-TCATKGCRTAGTTDGGRTAGT) (11). *mcrA* group b was amplified with specific primer pair AOM39_F (5′ GCTGTGTAGCAGGAGAG TCA) and AOM40_R (5′ GATTATCAGGTCACGCTCAC). PCR conditions for both target sequences were identical. The 50-μl amplification reaction mixtures contained 1 μl of template DNA, 41.5 μl of 1× buffer, 1 μl each of 10 μM forward and reverse primer, 2.5 U of TaqPlus Precision polymerase (Stratagene, La Jolla, Calif.), and 5 μl of 10 mM stock deoxynucleoside triphosphate mixture. Amplifications were carried out with the following profile: 94°C for 3 min, then 36 cycles of 94°C for 40 s, 55°C for 1.5 min, and 72°C for 2 min, followed by a final extension at 72°C for 10 min.

Clone library construction and sequencing. SSU rRNA and *mcrA* amplicons were visualized on 1% agarose gels in 1× TBE and purified directly with the Qiaquick PCR purification kit (Qiagen, Valencia, Calif.). Purified products from fosmid screening were sequenced directly (see below). Purified products from environmental samples and AMIS microcosm enrichment were cloned into the pCR4-Topo vector with a Topo TA cloning kit for sequencing (Invitrogen, Carlsbad, Calif.) and transformed by chemical transformation into TOP10 one shot cells according to the manufacturer's instructions. Transformants were transferred to 96-well plates containing 180 μl of LB containing 50 μg of kanamycin per ml and 7% glycerol and stored at −80°C.

TABLE 2. Archaeal 16s rDNA and *mcrA* clone recovery from MOA-containing sediments and fosmid DNA library[a]

DNA	Group	Recovery (no. of clones)					Total no. of clones
		Eel River		Monterey Canyon F17.1	AMIS microcosm C4.1	Blake Ridge PC26	
		T201	Gzfos				
Archaeal 16s rDNA	ANME-1	62	8	1		3	74
	ANME-2						
	ANME-2a	1				41	42
	ANME-2b	9					9
	ANME-2c	20	1	27	43		91
	Methanogen-like			1	1	22	24
	Other	6		49	31	5	91
mcrA group	a	13	4	9		25	51
	b	+	6	+		ND	6
	c	3	4	3	14	5	29
	d		1			3	4
	e			3			3

[a] T201 environmental sequences and the Gzfos library were both derived from the same purified cell preparation of MOA from Eel River T201 sediment (see text). Environmental samples and fosmid library were screened with universal *mcrA* primers ME-1 and ME-2 and ANME-1 type b-specific *mcrA* primers AOM39 and AOM40 (see text). +, positive amplification with AOM39 and AOM40 primer set. *mcrA* group represents conceptual translation product. ND, not determined.

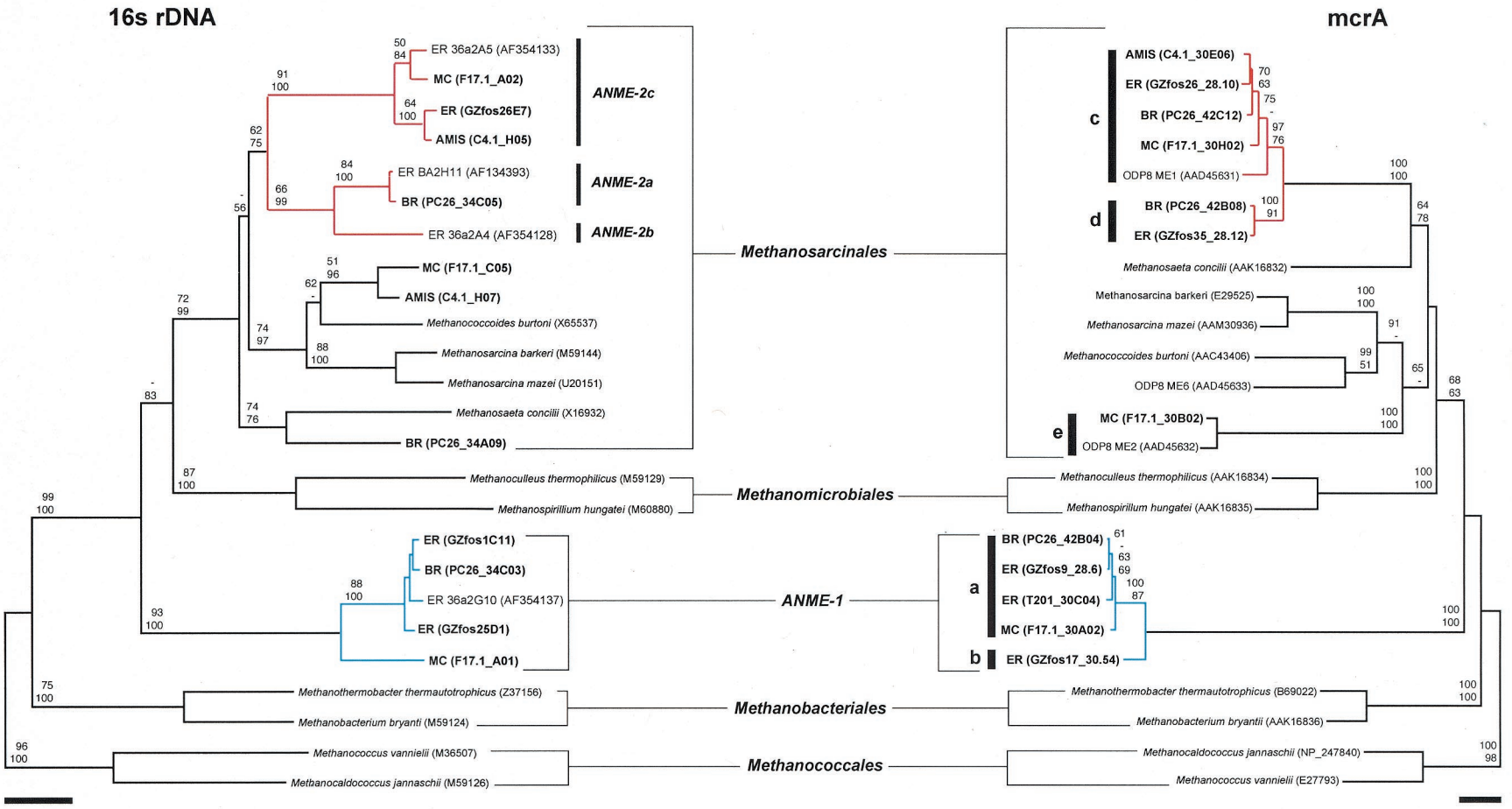

FIG. 1. Distance comparison of SSU rRNA and *mcrA*-based phylogenetic trees of environmental clones and primary methanogenic lineages. Bootstrap values are based on 1,000 replicates each (neighbor joining on top and parsimony on bottom) and are shown for branches with greater than 50% support. *Methanocaldococcus* spp. were used as the out group reference. ER, Eel River; MC, Monterey Canyon; AMIS, microcosm; BR, Blake Ridge. Boldface identifies clones identified and sequenced in this study. Red highlights ANME-2 group members, and blue highlights ANME-1 group members. Scale bars represent 0.05 nucleotide or amino acid substitution per site.

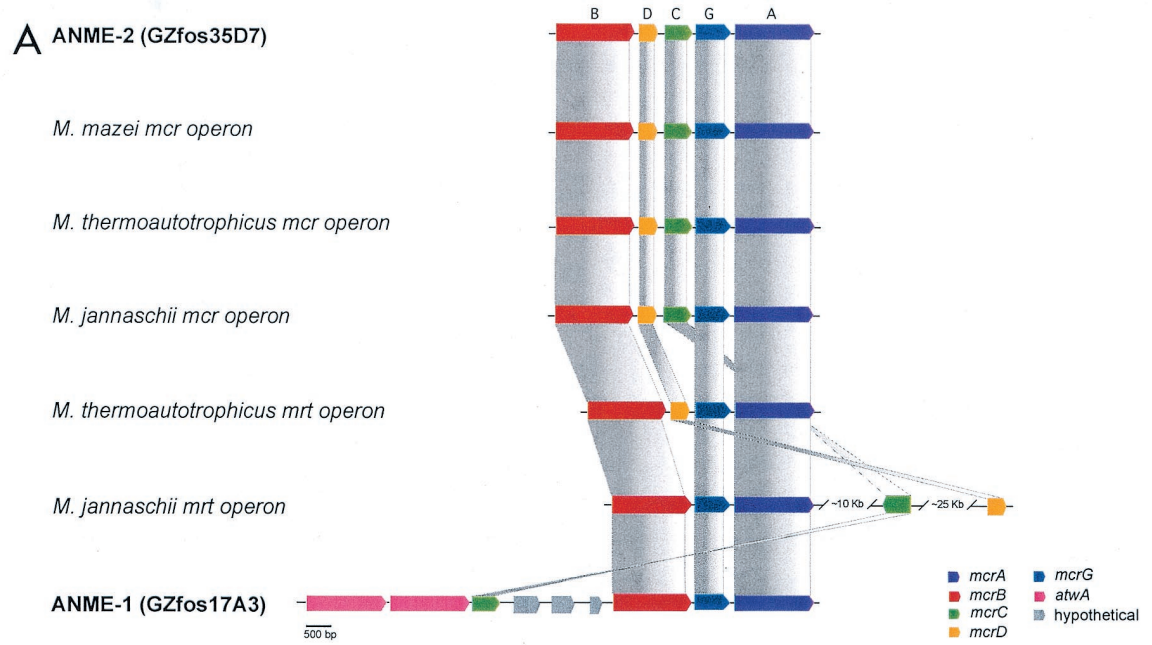
A
ANME-2 (GZfos35D7)
M. mazei mcr operon
M. thermoautotrophicus mcr operon
M. jannaschii mcr operon
M. thermoautotrophicus mrt operon
M. jannaschii mrt operon
ANME-1 (GZfos17A3)
B D C G A
~10 Kb
~25 Kb
500 bp
mcrA
mcrB
mcrC
mcrD
mcrG
atwA
hypothetical

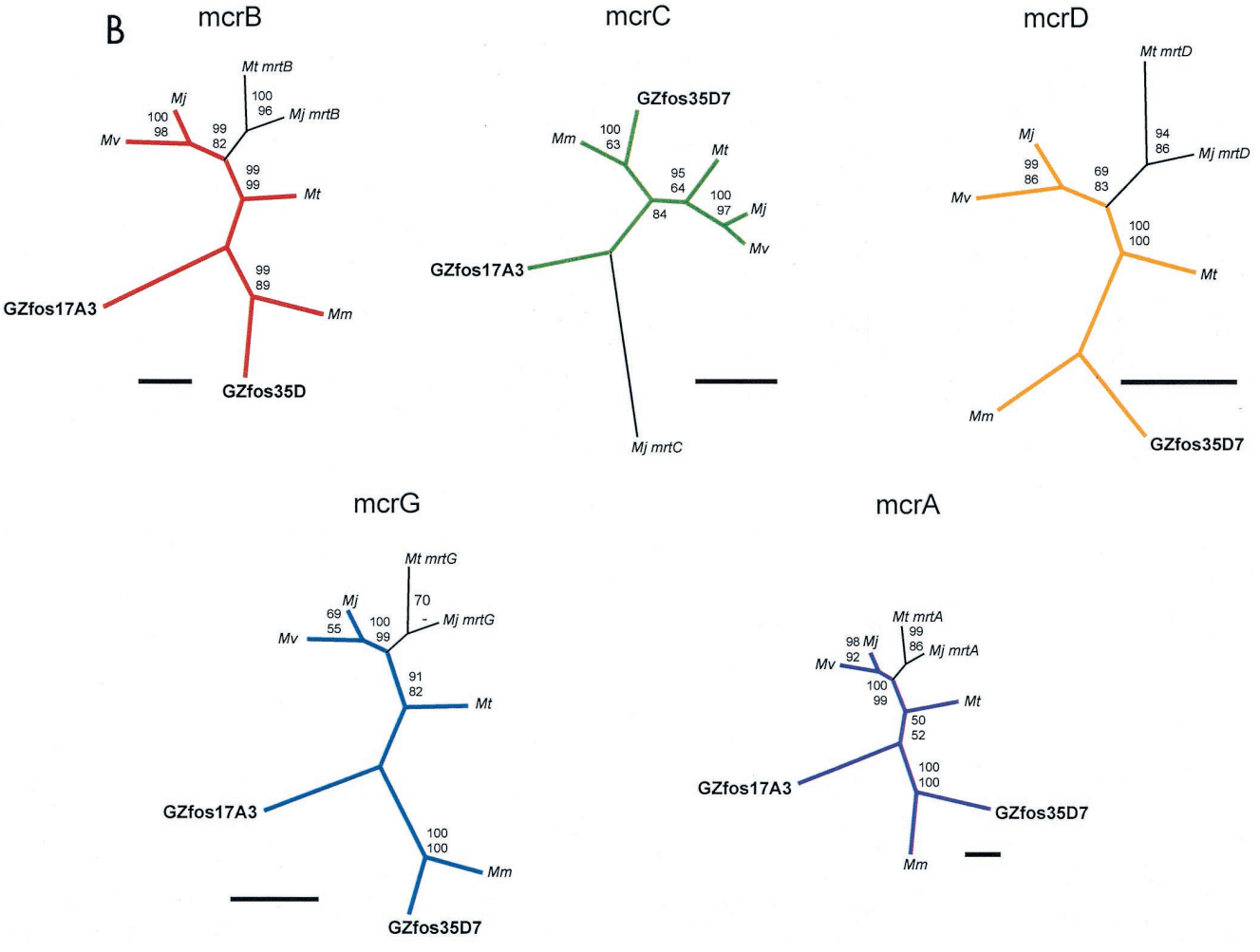
B
mcrB
Mt mrtB
Mj
Mj mrtB
Mv
Mt
GZfos17A3
Mm
GZfos35D
mcrC
GZfos35D7
Mm
Mt
Mj
Mv
GZfos17A3
Mj mrtC
mcrD
Mt mrtD
Mj
Mj mrtD
Mv
Mt
Mm
GZfos35D7
mcrG
Mt mrtG
Mj
Mj mrtG
Mv
Mt
GZfos17A3
Mm
GZfos35D7
mcrA
Mt mrtA
Mj
Mj mrtA
Mv
Mt
GZfos17A3
GZfos35D7
Mm

Plasmid DNA was purified from glycerol stocks with the Montage Plasmid Miniprep$_{96}$ kit (Millipore, Bedford, Mass.) following the manufacturer's protocol and stored at −20°C. Plasmid insert sequence data were collected on an ABI Prism 3100 DNA sequencer (Applied Biosystems Inc, Foster, Calif.) with Big Dye chemistry (PE Biosystems, Foster, Calif.) according to the manufacturer's instructions. Plasmids were sequenced bidirectionally with M13F and M13R primers. SSU rRNA and *mcrA* amplicons from fosmid screening were sequenced bidirectionally with the A20 and A958 and the AOM39 and AOM40 primer pairs, respectively. Sequences were edited manually from traces with Sequencher software version 4.1.2 (Gene Codes Corporation, Ann Arbor, Mich.).

Phylogenetic analysis. Phylogenetic analyses of SSU and *mcrA* sequences were preformed on sequences from known MOA groups, and representatives from the primary lines of descent within methanogenic groups. SSU rRNA sequence data were compiled with ARB software (www.arb-home.de) and aligned with sequences from the GenBank database with the FastAligner program. Aligned sequences were visually inspected for conservation of secondary structure features and manually edited when necessary. SSU rRNA trees were based on comparison of 541 nucleotides. Deduced amino acid sequences for environmental *mcrA* clones were determined from 684 bp of overlapping nucleotide sequence and aligned with the Clustal method implemented in MegAlign (DNA Star, Madison, Wis.). *mcrA* trees were based on comparison of 276 amino acids with the exception of *Methanosaeta concilii* (157 amino acids). Phylogenetic trees for both SSU rRNA and *mcrA* genes were generated with distance and parsimony methods implemented in PAUP version 4.0b10 (29). SSU rRNA sequence distances were estimated with the Kimura two-parameter model. Bootstrapping for distance and parsimony was accomplished with 1,000 replicates per tree with heuristic search methods.

Gene phylogenies for *mcrA* and *mrt* operon subunits were constructed from representative methanogenic lineages and two fosmids containing the complete *mcrA* operon from MOA groups ANME-1 and ANME-2 (Gzfos17A3 and Gzfos35D7). Alignments based on complete protein sequences were generated with the Clustal method implemented in MegAlign (DNA Star, Madison, Wis.). Unrooted trees for both *mcrA* and *mrt* subunits were generated with distance and parsimony methods implemented in PAUP version 4.0b10 (29). Bootstrapping for distance and parsimony was accomplished with 1,000 replicates per tree with heuristic search methods.

Nucleotide sequence accession numbers. *mcrA* and rRNA gene sequences were submitted to GenBank and have been assigned accession numbers AY324362 to AY324373 and AY324374 to AY324382, respectively. In addition, genomic DNA sequences from GZfos17A3 and GZfos35D7 containing the complete *mcrA* operon were submitted to GenBank and have been assigned accession numbers AY327048 and AY327049, respectively.

RESULTS

Detection of PCR-amplified *mcrA* sequence in anaerobic methane oxidation-associated samples. Samples were collected from marine sediments that were known to be active in anaerobic methane oxidation and that contained methanotrophic archaeal groups in different proportions. The AMIS bioreactor was also incorporated in the study because it enriched for the growth of specific MOA types. PCR-derived clone libraries containing a conserved region of the *mcrA* locus were generated (see Materials and Methods) and compared among and between anaerobic methane oxidation-associated environmental samples, methane-oxidizing microcosm enrichment (10a), and genomic libraries from purified MOA cell preparations (Table 1 and Materials and Methods).

A total of 93 deduced *mcrA* clones fell into five distinct groups, a to e (Table 2 and Fig. 1). Nucleotide sequence heterogeneity within each group was moderate, with the majority of polymorphic sites falling in third-codon positions. Amino acid sequence identity between representative group a and group b sequences was 92.5%, and 93.3% between representative group c and group d sequences. Based on these observations, group a, group b, group c, and group d were collapsed into groups a-b and c-d, respectively. Group a-b was on average 44.9% (±1.3%) identical to group c-d. Group e was on average 45.6% (±1.9%) identical to group a-b, and 59.6% (±0.3%) identical to group c-d. Compared to *mcrA* sequences from well-characterized methanogenic groups, *mcrA* group a-b was on average 44.6% (±2.9%) identical, group c-d was 63.6% (±1.8%) identical, and group e was 58.1% (±5.2%) identical.

Common *mcrA* groups were shared between locations. However, in two instances, a single group was associated with a specific sample or location. *mcrA* group e was detected solely in Monterey Canyon seep sediment, and only *mcrA* group c was detected in methane-oxidizing microcosm enrichment (Table 2). Taken together, these results indicate that *mcrA* genes are readily detectable in anaerobic methane oxidation sediments and that their sequence diversity is not uniformly distributed.

In order to assess *mcrA* amplification bias associated with degenerate primer screening (17) and to identify large-insert DNA clones (i.e., fosmids) for genomic analyses, PCR-derived *mcrA* clone recovery from Eel River environmental sample T201 was compared to clone recovery from a fosmid library constructed from T201 purified cell preparations. T201 provided a 4:1 clone ratio between group a and group c, compared to a 1:1 ratio in fosmid clones, despite a clear bias in ANME-1 SSU rRNA representation (Table 2). This pattern was repeated for other environmental samples containing both the a and c groups, suggesting a consistent amplification bias toward group a by the degenerate *mcrA* primers ME1 and ME-2 (Table 2).

Environmental distribution and phylogeny of MOA-associated *mcrA* sequences. Recent studies suggest that *mcrA* can substitute for SSU rRNA sequences in determining phylogenetic relationships between methanogenic archaea (18). To test this assertion and determine the phylogenetic affiliation of MOA-associated *mcrA* groups, SSU rRNA sequence recovery was compared to *mcrA* sequence recovery in the same samples.

FIG. 2. (A) Schematic depiction of *mcrA* and *mrt* operon structure for MOA-associated fosmids and major methanogenic lineages. The *mcrA* operon typically consists of *mcrBDCGA*. The *mrt* operon structure varies between lineages. Scale bar, 500 bp. (B) Gene trees for *mcrA* and *mrt* subunits depicted in A. Abbreviations for methanogenic species harboring these genes are Mj, *Methanocaldococcus jannaschii*; Mv, *Methanococcus vannielii*; Mt, *Methanothermobacter thermautotrophicus*; and Mm, *Methanosarcina mazei*. Accession numbers for sequences used in the analyses are shown in parentheses for *mcrB*-Mj (NP_247836.1), *mcrB*-Mv (P07956), *mcrB*-Mt (NP_276296.1), *mcrB*-Mm (NP_633268.1), *mcrC*-Mj (NP_247838.1), *mcrC*-Mv (P07960), *mcrC*-Mt (NP_276294.1), *mcrC*-Mm (NP_633266.1), *mcrD*-Mj (NP_247837.1), *mcrD*-Mv (P07957), *mcrD*-Mt (NP_276295.1), *mcrD*-Mm (NP_633267.1), *mcrG*-Mj (NP_247839.1), *mcrG*-Mv (P07963), *mcrG*-Mt (NP_276293.1), *mcrG*-Mm (NP_633265.1), *mcrA*-Mj (NP_247840.1), *mcrA*-Mv (E27793), *mcrA*-Mt (NP_276292.1), *mcrA*-Mm (NP_633264.1), *mrtB*-Mj (NP_247045.1), *mrtB*-Mt (NP_276260.1), *mrtC*-Mj (NP_247058.1), *mrtD*-Mj (NP_247083.1), *mrtD*-Mt (NP_276259.1), *mrtG*-Mj (NP_247046.1), *mrtG*-Mt (NP_276258.1), *mrtA*-Mj (NP_247047.1), and *mrtA*-Mt (NP_276257.1). Bootstrap values are based on 1,000 replicates each (neighbor joining on top and parsimony on bottom) and are shown for branches with greater than 50% support. Trees are unrooted. Scale bars represent 50 amino acid substitutions.

Most samples contained a high proportion of ANME-1 and ANME-2 SSU rRNA clones relative to other archaeal groups, although clone recovery varied between sites. Eel River T201, although dominated by ANME-1 sequences, also contained ribotypes corresponding to ANME-2a/b and ANME-2c (Table 2). Monterey Canyon sample F17.1, although dominated by ANME-2c sequences, also contained an ANME-1-like and a *Methanococcoides*-like sequence (Table 2). Similarly, methane-oxidizing microcosm C4.1 (10a) enriched from Monterey Canyon sediment was dominated by sequences corresponding to ANME-2c, but also contained a methanogen-like sequence most similar to *Methanococcoides* spp. (Table 2). Nonetheless, the vast majority of SSU rRNA clones recovered from these Monterey Canyon and Eel River samples designated other (data not shown) failed to group with any bona fide methanogen group (Table 2 and data not shown). In contrast, Blake Ridge PC26, although dominated by ANME-2a, also contained a common methanogen-like ribotype corresponding to *Methanosaeta* spp. (Table 2 and Fig. 1).

Phylogenetic trees constructed for *mcrA* and SSU rRNA sequences recovered from the same samples exhibited a high degree of congruence, enabling tentative assignment of MOA-associated *mcrA* groups to specific archaeal lineages (see Materials and Methods). The *mcrA* group a-b was associated with the ANME-1 lineage, while group c-d was associated with the ANME-2 lineage (Fig. 1). ANME-2a/b and ANME-2c rRNA genes formed a monophyletic group within the *Methanosarcinales* (Fig. 1). Similarly, *mcrA* group c-d, along with environmental sample ODP8-ME1 (3), formed a monophyletic cluster most closely related to *Methanosaeta concilii* (Fig. 1). The *mcrA* group e fell within the *Methanosarcinales*. (Fig. 1). The absence of ANME-1 in the methane-oxidizing microcosm enrichment (10a) provided independent support for the associations inferred from SSU rRNA and *mcrA* tree topologies. Consistent with this observation, all but one SSU rRNA clone and all *mcrA* clones retrieved from the methane-oxidizing enrichment fell within the ANME-2c subdivision and *mcrA* group c, respectively (Table 2 and Fig. 1). The *mcrA* group e, recovered only in Monterey Canyon, putatively fell within the *Methanococcoides* along with ODP8-ME2 and ODP8-ME6, based on SSU rRNA tree topology (Table 2 and Fig. 1).

To better define the evolutionary origin of MOA-associated *mcrA* groups described above, sequence alignments containing both methyl coenzyme M reductase (*mcrA*) and methyl coenzyme M reductase II (*mrt*) subunits from *Methanocaldococcus jannaschii*, *Methanococcus vannielii*, *Methanthermobacter thermoautotrophicus*, and *Methanosarcina mazei* were compared to the homologous genes in MOA-associated environmental PCR clones and fosmids. Sequence identity between the common region of *mcrA* and *mrtA* in *M. jannaschii* and *M. thermoautotrophicus* was 80.2% and 76.6%, respectively. The *mrtA* sequence identity between *M. jannaschii* and *M. thermautotrophicus* was 84.7%. In contrast, ANME-1-affiliated *mcrA* group a-b was on average 47.3% (±1.3%) identical to *M. jannaschii* and 48.6% (±1.3%) identical to *M. thermoautotrophicus mrtA*. The ANME-2-affiliated *mcrA* group c-d was on average 57.5% (±0.9%) identical to *M. jannaschii* and 57.9% (±3.7%) identical to *M. thermoautotrophicus mrtA*.

The *mrt* locus is found in both the *Methanococcales* and *Methanobacteriales* lineages and represents a second, genetically distinct *mcrA* operon with alternative subunit composition and order (Fig. 2A) (16, 27). In contrast, members of the *Methanosarcinales* contain only the *mcrA* locus, based on analysis of several completed genomes (9, 27). From a phylogenetic perspective, *mrtA* sequences form a related group within the *Methanococcales mcrA* lineage (16, 18). The subunit composition and order of ANME-2-associated fosmid GZfos35D7 resembled the *mcrA* structure found in all methanogenic lineages (*mcrBDCGA*) (Fig. 2A). In contrast, the subunit composition and order of ANME-1-associated fosmid GZfos17A3 appeared to diverge from canonical *mcrA* structure by the loss of *mcrD* and rearrangment of *mcrC* (Fig. 2A). No *mcrD* homolog could be deduced from the entire range of 37,609 contiguous bp carried by GZfos17A3.

Although the pattern of rearrangement observed for the GZfos17A3 *mcrA* operon resembles that of *mrt* operons in *M. jannaschii* and *M. thermoautotrophicus*, analysis of homology between individual GZfos17A3 subunits is consistent with *mcrA* affiliation (Fig. 2B). The *mrt* subunits from *M. jannaschii* and *M. thermoautotrophicus* were most closely related to the respective *mcrA* paralogs and formed subdivisions within each group (Fig. 2B). MOA-associated *mcrA* subunits grouped consistently within the major *mcrA* groups and not with *mrt* subdivisions (Fig. 2B). In addition, all *mcrA* subunits from ANME-2-associated fosmid GZfos35D7 grouped with their *M. mazei* cognates, consistent with the SSU rRNA and *mcrA* phylogeny shown in Fig. 1 (Fig. 2B).

Conservation of active-site amino acids in MOA *mcrA* groups. The conservation of primary structure relevant to catalytic activity in MOA *mcrA* groups was evaluated by comparing conserved amino acid residues among groups a to e and several methanogenic lineages (Fig. 3). The crystal structure of *mcrA* from *Methanothermobacter thermoautotrophicus* was used as a reference (6). Within the coverage area of MOA-associated *mcrA* groups, the structure of *mcrA* from *M. thermoautotrophicus* exhibits 11 conserved amino acids involved in active-site function. These include five methyl-modified amino acids, H257, R271, Q400, C452, and G445, four cofactor F_{430} interacting amino acids, F330, Y333, F443, and Y444, and two additional coenzyme B binding amino acids, K256 and A272 (6).

A second *mcrA* crystal structure determined for a phylogenetically distant methanogen, *Methanosarcina barkeri*, reveals marked conservation of these amino acids and their modifications except for the Q147 methyl modification and a substitution, Y444 to F (10). In contrast, among the many conserved sites, MOA-associated *mcrA* group a contained two amino acid substitutions, converting Q400 to V and R270 to K. Group b contained four amino acid substitutions, converting Q400 to V, C452 to A, R270 to K, and Y444 to F. Groups c to e contained a single amino acid substitution, converting Y444 to F. Given that *mcrA* from *M. barkeri* is catalytically active, the Y444 to F substitution common to groups b to e appears to be neutral in terms of protein function, a supposition supported by parallel substitution in other methanogenic lineages (Fig. 3 and data not shown).

MOA-associated *mcrA* groups a to d contained a high proportion of cysteine residues compared to other methanogenic lineages. Within the conserved coverage area, cysteine accounted for 1.79% of residues in *M. thermoautotrophicus*,

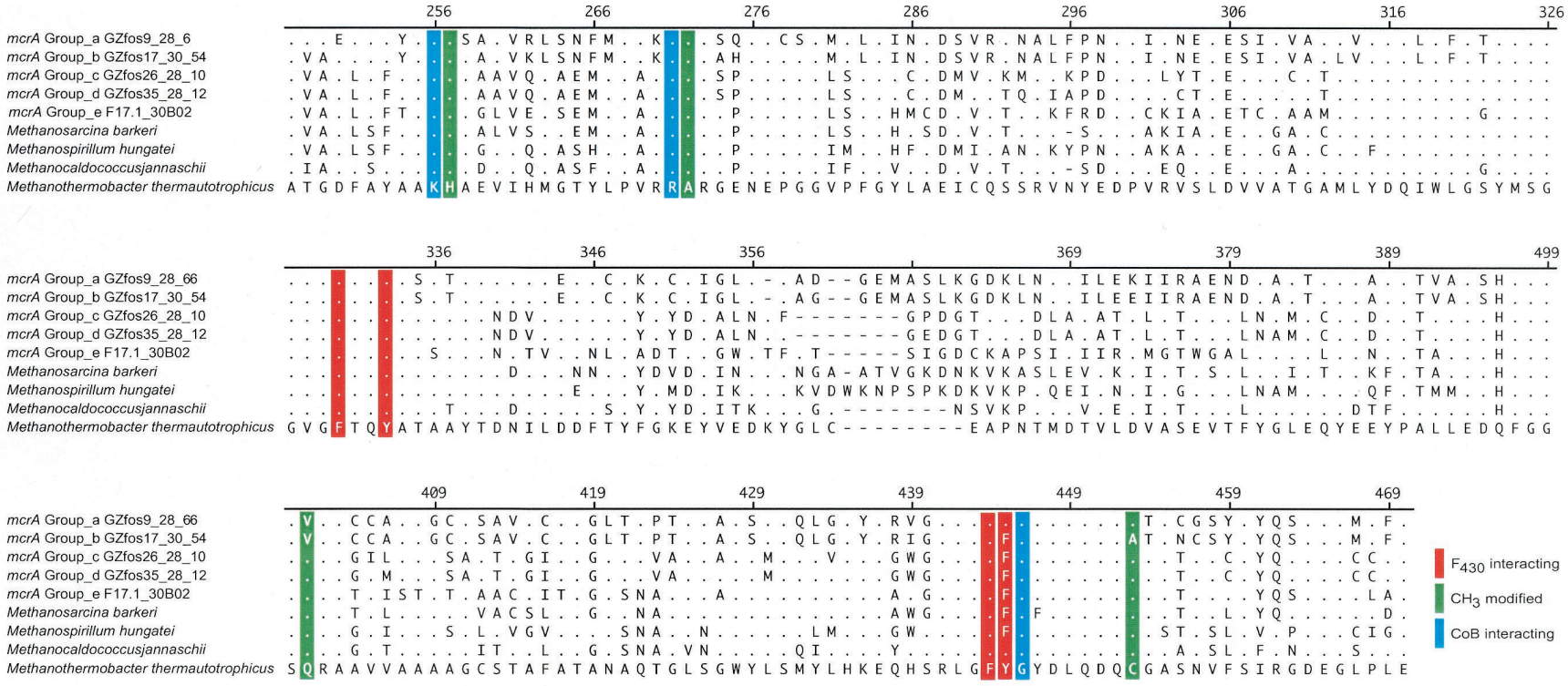

FIG. 3. Amino acid alignment of representative environmental *mcrA* types and primary methanogenic lineages. *Methanothermobacter thermoautotrophicus* was used as the reference sequence (GenBank U10036). Position numbers correspond to the reference sequence. Amino acid identity at a given position is denoted by dots, and gaps are marked by dashes. Conserved amino acids are coded by color according to predicted CH_3 modification (green), F_{430} binding (red), or coenzyme B interaction (blue).

1.31% in *M. barkeri*, 0.9% in *Methanocaldococcus jannaschii*, and 1.3% in *Methanospirillium hungatei* (Fig. 3). In contrast, cysteine accounted for 3.95% of residues in *mcrA* group a, 3.07% in group b, 3.57% in group c, 4.02% in group d, and 2.65% in group e.

DISCUSSION

Identification of *mcrA* in MOA. In total, our data suggest that *mcrA* genes are present in MOA groups and discernible from those of other methanogenic archaea. Two *mcrA* groups (a and b) correspond to ANME-1, and two *mcrA* groups (c and d) correspond to ANME-2, identifications that are based on four types of evidence. First, variation in the representation of ANME-1 and ANME-2 ribotypes in three separate natural MOA populations, Monterey Canyon, Eel River, and Blake Ridge, suggested rough correlation between specific *mcrA* groups and specific ANME ribotypes. Second, congruence between *mcrA* and SSU rRNA tree topologies was indicative of *mcrA* group affiliation relative to SSU rRNA relationships among known methanogenic and methane-oxidizing archaeal lineages. Third, only *mcrA* group c sequences were recovered from a methane-oxidizing microcosm containing only a single MOA type, ANME-2c. Finally, fosmids representing *mcrA* groups a to d were identified from libraries derived from Eel River T201 cell preparations enriched for ANME-1 and ANME-2 (Hallam et al., unpublished data). The *mcrA* sequence identity within the methane-oxidizing ANME-1 and ANME-2 groups raises several questions relating to the origin, evolution, and function of methanogenic genes in MOA.

Evolution and divergence of MOA-associated *mcrA* genes. The parallel distribution of ANME-1 and ANME-2 *mcrA* groups in two closely related subdivisions, a-b and c-d, raises the formal possibility of *mcrA* operon duplication or gene transfer within each lineage. For example, within the deeper branching *Methanobacteriales* and *Methanococcales* lineages, phylogenetic studies suggest that the *mcrA* operon paralog *mrt* originated in the *Methanococcales* and was subsequently transferred to a member of the *Methanobacteriales* (15, 20). Comparison of a-b and c-d MOA-associated *mcrA* groups to *mrtA* is inconsistent with the lateral gene transfer of this locus into MOA groups. MOA-associated *mcrA* sequences grouped consistently among themselves and with *mcrA* sequences from other lineages.

These observations are further supported by comparison of the complete *mcrA* operon from two fosmids representing *mcrA* group d (ANME-2, GZfos35D7) and b (ANME-1, GZfos17A3). The *mcrA* subunits from both fosmids consistently grouped with homologous *mcrA* subunits and not with the corresponding *mrt* subunits, with the possible exception of the *mcrC* subunit from GZfos17A3. In ANME-2, the canonical *mcrA* operon structure *mcrBDCDGA* was conserved and, combined with gene similarities, appears to reflect descent from a common *Methanosarsinales* ancestor, consistent with rRNA phylogenetic relationships. In contrast, in ANME-1 there was a significant deviation from this gene order and arrangement, more similar to that found in the *M. jannaschii mrt* structure, with *mrcC* located several kilobases upstream of *mcrBGA*. This may reflect functional as well as evolutionary differences between the ANME-1 and ANME-2 MOA groups.

Structure-function comparison of MOA and methanogen *mcrA* genes. Comparison of active-site amino acids suggests that MOA-associated *mcrA* groups c-d and e may have the potential to catalyze the terminal step in methanogenesis. In contrast, *mcrA* group a-b harbors substitutions in universally conserved residues subject to methyl modification, including Q400 and C472. Residue Q400, located in the vicinity of cofactor F430, plays an important role in active-site geometry (6, 10). Although methyl modification of Q400 does not appear to be essential (10), substitution of residue Q400 with V in *mcrA* group a-b could alter active-site geometry and therefore protein function. The methyl moiety of C472, although outside the active site, forms two hydrophobic interactions with the side chains of H382 of McrB and L468 of McrA (6, 10). Changing C472 to A in *mcrA* group b may affect the geometry of these interactions.

Given these changes, the catalytic potential of group a-b is more uncertain from the standpoint of canonical methanogenesis. Despite the group a-b substitutions, the very presence of *mcrA* genes in MOA suggests activation of one or more elements in the methanogenic pathway. Although at present no known biological mechanism for anaerobic methane cleavage has been identified, biochemical models suggest that anaerobic activation of the methane C-H bond via *mcrA* could theoretically occur by the formation of an adduct between F430 (nickel porphyrin) and the radical mercaptoheptanoyl threonine phosphate (2, 13). This is consistent with physiological studies that suggest that methanogens are capable of simultaneous production and low-level oxidation of methane under anaerobic conditions (34, 35). Relevant here is the observation that both methane production and oxidation were equally inhibited by the substrate analog 2-bromoethanesulfonic acid, a potent inhibitor of *mcrA* function (34, 35).

Genomic potential of methanogenic pathway genes in MOA. Our results show that MOA contain one of the essential and diagnostic genes of the methanogenic pathway, even though environmental evidence suggests that MOA consume but do not necessarily produce methane. The identification of these genes provides a means to identify ANME group members on the basis of *mcrA* sequence. Moreover, identification of MOA-associated *mcrA* groups defines a functional genomic link between methanogenic and putative reverse methanogenic archaea. Ongoing genomic analysis of fosmid libraries derived from Eel River T201 cell preparations have identified numerous operons containing methanogenic genes, including formylmethaneofuran dehydrogenases, formyltransferases, cyclohydrolases, F420-reducing dehydrogenases, and methyltransferases. These observations provide strong support for the hypothesis that MOA may have co-opted key elements of the methanogenic pathway to enable an anaerobic methanotrophic lifestyle (Hallam et al., unpublished data). Specific questions relating to methanogenic protein function in MOA await further genomic, biochemical, structural, and proteomic analysis.

ACKNOWLEDGMENTS

Special thanks to Victoria Orphan, Bill Ussler, and Charlie Paull for providing Blake Ridge sediment core samples, to David Graham for providing valuable scientific commentary, to Lynne Christianson at MBARI and the Joint Genome Institute staff for providing technical support, to all the pilots of the ROVs *Ventana* and *Tiburon* and the

crews on board the R/V *Point Lobos*, R/V *Western Flyer*, and R/V *Cape Hatteras*.

This study was supported by the David and Lucille Packard Foundation. Part of this work was performed under the auspices of the U.S. Department of Energy's Office of Science, Biological and Environmental Research Program and the University of California, Lawrence Livermore National Laboratory, under contract no. W-7405-Eng-48, Lawrence Berkeley National Laboratory under contract no. DE-AC03-765F00098, and Los Alamos National Laboratory under contract no. W-7405-ENG-36.

REFERENCES

1. **Barnes, R. O., and E. D. Goldberg.** 1976. Methane production and consumption in anaerobic marine sediments. Geology **4:**297–300.
2. **Berkessel, A.** 1991. Methyl-coenzyme M reductase: model studies on pentadentate nickel complexes and a hypothetical mechanism. Bioorg. Chem. **19:**101–115.
3. **Bidle, K. A., M. Kastner, and D. H. Bartlett.** 1999. A phylogenetic analysis of microbial communities associated with methane hydrate containing marine fluids and sediments in the Cascadia margin (ODP site 892B). FEMS Microbiol Lett. **177:**101–108.
4. **Boetius, A., K. Ravenschlag, C. J. Schubert, D. Rickert, F. Widdel, A. Gieseke, R. Amann, B. B. Jorgensen, U. Witte, and O. Pfannkuche.** 2000. A marine microbial consortium apparently mediating anaerobic oxidation of methane. Nature **407:**623–626.
5. **Ellermann, J., R. Hedderich, R. Bocher, and R. K. Thauer.** 1988. The final step in methane formation. Investigations with highly purified methyl-CoM reductase (component C) from Methanobacterium thermoautotrophicum (strain Marburg). Eur. J. Biochem. **172:**669–677.
6. **Ermler, U., W. Grabarse, S. Shima, M. Goubeaud, and R. K. Thauer.** 1997. Crystal structure of methyl-coenzyme M reductase: the key enzyme of biological methane formation. Science **278:**1457–1462.
7. **Ferry, J. G.** 1992. Biochemistry of methanogenesis. Crit. Rev. Biochem. Mol. Biol. **27:**473–503.
8. **Ferry, J. G.** 1999. Enzymology of one-carbon metabolism in methanogenic pathways. FEMS Microbiol. Rev. **23:**13–38.
9. **Galagan, J. E., C. Nusbaum, A. Roy, M. G. Endrizzi, P. Macdonald, W. FitzHugh, S. Calvo, R. Engels, S. Smirnov, D. Atnoor, A. Brown, N. Allen, J. Naylor, N. Stange-Thomann, K. DeArellano, R. Johnson, L. Linton, P. McEwan, K. McKernan, J. Talamas, A. Tirrell, W. Ye, A. Zimmer, R. D. Barber, I. Cann, D. E. Graham, D. A. Grahame, A. M. Guss, R. Hedderich, C. Ingram-Smith, H. C. Kuettner, J. A. Krzycki, J. A. Leigh, W. Li, J. Liu, B. Mukhopadhyay, J. N. Reeve, K. Smith, T. A. Springer, L. A. Umayam, O. White, R. H. White, E. Conway de Macario, J. G. Ferry, K. F. Jarrell, H. Jing, A. J. Macario, I. Paulsen, M. Pritchett, K. R. Sowers, R. V. Swanson, S. H. Zinder, E. Lander, W. W. Metcalf, and B. Birren.** 2002. The genome of M. acetivorans reveals extensive metabolic and physiological diversity. Genome Res. **12:**532–542.
10. **Grabarse, W., F. Mahlert, S. Shima, R. K. Thauer, and U. Ermler.** 2000. Comparison of three methyl-coenzyme M reductases from phylogenetically distant organisms: unusual amino acid modification, conservation and adaptation. J. Mol. Biol. **303:**329–344.

10a. **Girguis, P. R., V. J. Orphan, S. J. Hallam, and E. F. Delong.** 2003. Growth and methane oxidation rates of anaerobic methanotrophic archaea in a continuous-flow bioreactor. Appl. Environ. Microbiol. **69:**AEM 515–03.

11. **Hales, B. A., C. Edwards, D. A. Ritchie, G. Hall, R. W. Pickup, and J. R. Saunders.** 1996. Isolation and identification of methanogen-specific DNA from blanket bog peat by PCR amplification and sequence analysis. Appl Environ Microbiol. **62:**668–675.
12. **Hinrichs, K. U., J. M. Hayes, S. P. Sylva, P. G. Brewer, and E. F. DeLong.** 1999. Methane-consuming archaebacteria in marine sediments. Nature **398:** 802–805.
13. **Hoehler, T. M., and M. J. Alperin.** 1996. Anaerobic methane oxidation by a methanogen-sulfate reducer consortium: geochemical evidence and biochemical considerations, p. 326–333. *In* M. E. Lidstrom and F. R. Tabita (ed.), Microbial growth on C_1 compounds. Kluwer, Dordrecht, The Netherlands.
14. **Joye, S. B., T. L. Connell, L. G. Miller, R. S. Oremland, and R. S. Jellison.** 1999. Oxidation of ammonia and methane in an alkaline, saline lake. Limnol. Oceanogr. **44:**178–188.
15. **Lehmacher, A., and H. P. Klenk.** 1994. Characterization and phylogeny of mcrII, a gene cluster encoding an isoenzyme of methyl coenzyme M reductase from hyperthermophilic Methanothermus fervidus. Mol. Gen. Genet. **243:**198–206.
16. **Lueders, T., K. J. Chin, R. Conrad, and M. Friedrich.** 2001. Molecular analyses of methyl-coenzyme M reductase alpha-subunit (*mcrA*) genes in rice field soil and enrichment cultures reveal the methanogenic phenotype of a novel archaeal lineage. Environ. Microbiol. **3:**194–204.
17. **Lueders, T., and M. W. Friedrich.** 2003. Evaluation of PCR amplification bias by terminal restriction fragment length polymorphism analysis of small-subunit rRNA and *mcrA* genes by with defined template mixtures of methanogenic pure cultures and soil DNA extracts. Appl. Environ. Microbiol. **69:**320–326.
18. **Luton, P. E., J. M. Wayne, R. J. Sharp, and P. W. Riley.** 2002. The *mcrA* gene as an alternative to 16S rRNA in the phylogenetic analysis of methanogen populations in landfill. Microbiology **148:**3521–3530.
19. **Martens, C. S., D. B. Albert, and M. J. Alperin.** 1999. Stable isotope tracing of anaerobic methane oxidation in the gassy sediments of Eckernforde Bay, German Baltic Sea. Am. J. Sci. **299:**589–610.
20. **Nolling, J., A. Elfner, J. R. Palmer, V. J. Steigerwald, T. D. Pihl, J. A. Lake, and J. N. Reeve.** 1996. Phylogeny of *Methanopyrus kandleri* based on methyl coenzyme M reductase operons. Int. J. Syst. Bacteriol. **46:**1170–1173.
21. **Orphan, V. J., K. U. Hinrichs, W. Ussler, 3rd, C. K. Paull, L. T. Taylor, S. P. Sylva, J. M. Hayes, and E. F. Delong.** 2001. Comparative analysis of methane-oxidizing archaea and sulfate-reducing bacteria in anoxic marine sediments. Appl. Environ. Microbiol. **67:**1922–1934.
22. **Orphan, V. J., C. H. House, K. U. Hinrichs, K. D. McKeegan, and E. F. DeLong.** 2001. Methane-consuming archaea revealed by directly coupled isotopic and phylogenetic analysis. Science **293:**484–487.
23. **Orphan, V. J., C. H. House, K. U. Hinrichs, K. D. McKeegan, and E. F. DeLong.** 2002. Multiple archaeal groups mediate methane oxidation in anoxic cold seep sediments. Proc. Natl. Acad. Sci. USA **99:**7663–7668.
24. **Pancost, R. D., J. S. Sinninghe Damste, S. de Lint, M. J. van der Maarel, and J. C. Gottschal.** 2000. Biomarker evidence for widespread anaerobic methane oxidation in Mediterranean sediments by a consortium of methanogenic archaea and bacteria. The Medinaut Shipboard Scientific Party. Appl. Environ. Microbiol. **66:**1126–1132.
25. **Reeburgh, W. S.** 1976. Methane consumption in Caraico Trench waters and sediments. Earth Planet. Sci. Lett. **28:**337–344.
26. **Reeburgh, W. S.** 1996. Microbial growth on C_1 compounds. Kluwer Academic Publishers, Dordrecht, The Netherlands.
27. **Reeve, J. N., J. Nolling, R. M. Morgan, and D. R. Smith.** 1997. Methanogenesis: genes, genomes, and who's on first? J. Bacteriol. **179:**5975–5986.
28. **Stein, J. L., T. L. Marsh, K. Y. Wu, H. Shizuya, and E. F. DeLong.** 1996. Characterization of uncultivated prokaryotes: isolation and analysis of a 40-kilobase-pair genome fragment from a planktonic marine archaeon. J. Bacteriol. **178:**591–599.
29. **Swafford, D. L.** 2000. Phylogenetic analysis with parsimony (and other methods), version 4.0b10. Sinauer Associates, Sunderland, Mass.
30. **Thauer, R. K.** 1998. Biochemistry of methanogenesis: a tribute to Marjory Stephenson. 1998 Marjory Stephenson Prize Lecture. Microbiology **144:** 2377–2406.
31. **Valentine, D. L.** 2002. Biogeochemistry and microbial ecology of methane oxidation in anoxic environments: a review. Antonie Van Leeuwenhoek **81:**271–282.
32. **Valentine, D. L., and W. S. Reeburgh.** 2000. New perspectives on anaerobic methane oxidation. Environ. Microbiol. **2:**477–484.
33. **Whiticar, M. J., E. Faber, and M. Schoell.** 1986. Biogenic methane formation in marine and freshwater environments: CO_2 reduction vs. acetate fermentation-isotope evidence. Geochim. Cosmochim. Acta **50:**693–709.
34. **Zehnder, A. J., and T. D. Brock.** 1979. Biological energy production in the apparent absence of electron transport and substrate level phosphorylation. FEBS Lett. **107:**1–3.
35. **Zehnder, A. J., and T. D. Brock.** 1979. Methane formation and methane oxidation by methanogenic bacteria. J. Bacteriol. **137:**420–432.